35th Annual International Conference of the IEEE EMBS
Osaka, Japan, 3 - 7 July, 2013

A Working Heart-Brainstem Preparation of the Rat for the Study of Reflex Mediated Autonomic Influences on Atrial Arrhythmia Development

Jesse L. Ashton[1], Julian F. R. Paton[2], Mark L. Trew[1], Ian J. LeGrice[3], Bruce H. Smaill[1,3]

Abstract— **Vagal nerve activity has been shown to play a role in the formation and maintenance of atrial fibrillation (AF). Nerves on the atria are now increasingly being targeted using ablation-based therapies for the treatment of paroxysmal AF. *In vivo*, changes in vagal activity are part of an integrated autonomic profile that invariably involves accompanying modulations in sympathetic activity. To date, it has not been possible to replicate endogenous profiles of autonomic activity with the experimental set-ups used to study the effects of vagal stimulation on AF development. In this paper, we describe an experimental set-up using an *in situ* preparation that addresses these challenges for the first time. A high resolution surface electrode array has been used to make recordings of atrial electrograms during baroreflex activation from a preparation with intact innervation from brainstem to heart. This provides a novel framework for relating reflex-mediated autonomic activity to altered regional impulse propagation and electrical rhythm in the atria.**

I. Introduction

Clinical [1] and experimental [2] observations indicate autonomic nerve activity facilitates the induction and maintenance of atrial fibrillation (AF). Conditions that favour AF, namely significant shortening of atrial refractory periods [3] and increases in the rate of activation during AF [4], result from electrical stimulation of the vagus nerve and local stimulation of atrial nerves. Radiofrequency catheter ablation is routinely used to treat atrial arrhythmias and there has been suggestion that collateral denervation may contribute to the success of this procedure [5]. However, there have been conflicting reports on the impact of atrial denervation on AF [6], [7] so the role of the autonomic nervous system (ANS) in AF remains controversial.

The ANS constantly modulates heart rate, contractility and conduction to optimise cardiac output through reflex activation. For example, transient increases in blood pressure induce baroreflex mediated vagal activity that reduces heart rate and contractility. Baroreflex hyper-sensitivity has been associated with increased dispersion of effective refractory periods in patients with paroxysmal AF [8]. The majority of experimental studies investigating the influence of autonomic activity on atrial arrhythmias employ direct nerve stimulation. In order to establish the mechanisms by which endogenous autonomic activity can trigger arrhythmias or increase the risk of arrhythmia formation, it is necessary to develop new experimental approaches. We have developed an experimental set-up that contributes a significant step forward in addressing these challenges. In this paper we describe the use of an *in situ* artificially perfused rat preparation with intact ANS from brainstem to heart to make recordings of atrial conduction during autonomic reflex activation.

[1]Auckland Bioengineering Institute, University of Auckland, New Zealand.
[2]School of Physiology & Pharmacology, Bristol Heart Institute, University of Bristol, England.
[3]Department of Physiology, University of Auckland, New Zealand.
Corresponding author: J. L. Ashton (+64-9-373-7599x81495; e-mail: jash042@aucklanduni.ac.nz).

II. Methods

A. Working heart-brainstem preparation

All experiments were performed in accordance with the New Zealand Animal Welfare Act 1999 and approved by our Institutional Animal Ethics Committee. The working heart-brainstem preparation (WHBP) has been described previously [9] but this is the first time the WHBP has been extended and developed for the study of arrhythmia mechanisms. Sprague Dawley rats, 3-5 weeks old (45-110 g), were anaesthetised deeply with isoflurane until loss of paw withdrawal reflex. Animals were bisected below the diaphragm, exsanguinated, submerged in ice-cold Ringer solution (composition in mmol: 125 NaCl, 24 $NaHCO_3$, 5 KCl, 2.5 $CaCl_2$, 1.25 $MgSO_4$, 1.25 KH_2PO_4 and 10 D-glucose, pH 7.3 after carbogenation(5% CO_2 and 95% O_2)), decerebrated at the precollicular level and skinned.

A double-lumen cannula (ø 1.25 mm, DLR-4, Braintree Scientific, MA, USA) was inserted into the descending aorta for retrograde perfusion. Perfusion was reinstated using a peristaltic pump (520S, Watson Marlow, UK) with carbogenated Ringer solution warmed to 31 °C containing the oncotic agent Ficoll-70 (1.25%, Sigma Aldrich). Perfusion pressure (PP) was monitored using a pressure transducer (P23db, Gould Statham, CA, USA) connected to the second lumen of the cannula.

The left phrenic nerve was severed at the diaphragm and discharge was recorded from its proximal end using a bipolar glass suction electrode. Recordings were amplified and filtered (0.05-10 kHz, University of Auckland, NZ). A standard bipolar electrocardiogram (ECG) was recorded from leads attached to the forelimbs and sides of the thorax. The ECG was amplified and filtered (0.05-3 kHz, LP122, Grass Technologies, RI, USA) and acquired at 10 kHz along with PP and phrenic nerve signals using a PCI-6221 data acquisition card (National Instruments, TX, USA). Instantaneous heart rate (HR) in beats per minute (bpm)

978-1-4577-0216-7/13/$26.00 ©2013 IEEE

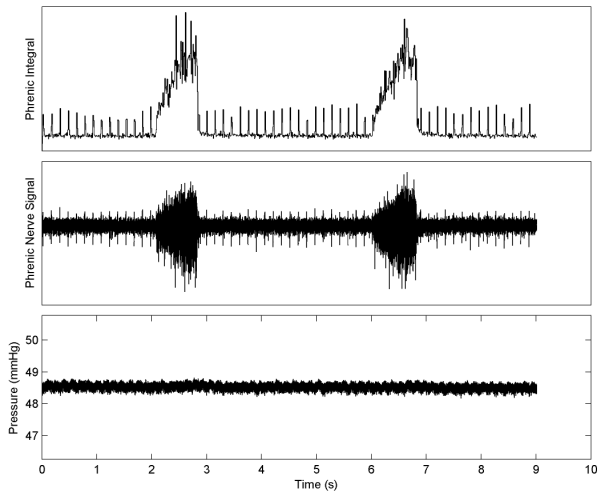

Fig. 1. **Ramp profile of the phrenic nerve signal integral characteristic of a normal eupnoeic pattern of respiration.** Integral calculated using intervals of 100 samples.

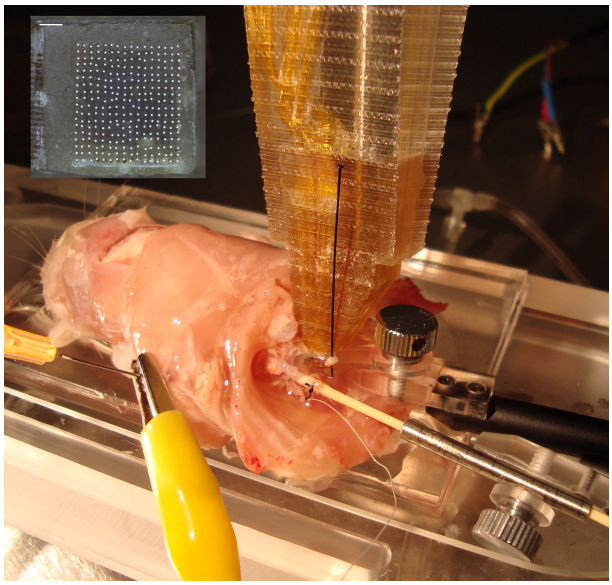

Fig. 2. **Electrode array**. Image shows the electrode array in position over the posterior right atrium of the working heart-brainstem preparation. The inset panel is a high magnification image of the electrode array recording surface. (Scale bar: 1 mm).

was derived by detecting R waves in the ECG identified using wavelet based peak detection implemented in LabView (National Instruments, TX, USA). A rectified integral of the phrenic nerve signal was calculated using intervals of 50-100 samples.

The perfusate flow was gradually increased (over a few minutes) from about 15 ml/min to a typical baseline flow of between 20 and 25 ml/min. Vasopressin (acetate salt, Sigma Aldrich) was added to the perfusate (final concentration 1.25-2.5 nmol) during this period to increase vascular resistance and PP. Rhythmic respiratory muscle contractions were seen after 1-5 minutes signaling the return of brainstem function as the mean PP reached a typical value of 50-70 mmHg. A muscle relaxant, vercuronium bromide, was added to the perfusate to suppress the respiratory movement (2-4 µg/ml, Sigma Aldrich). Flow was adjusted further until the phrenic signal integral attained a characteristic ramp profile (Fig. 1). This is referred to as an augmenting, eupnoeic pattern of respiration and indicates the brainstem is adequately perfused [9].

B. Electrode array construction

Atrial electrical activity was recorded using a custom designed and built array carrying 244 equispaced unipolar electrodes (250 µm spacing) spanning an area of approximately 5 x 4.6 mm^2. Polyimide insulated silver wire (uninsulated diameter of 75 µm) was threaded through wire guides with an array of holes (ø 100 µm) cut from 1 mm thick acrylic using a laser cutter (Speedy 300, Trotec, MI, USA). A mould to encase the wires and wire guide was printed in 3D (Dimension Elite, Stratasys, MN, USA) and then filled with resin (Procure 812, ProSciTech Pty Ltd, Qld, Australia) and cured at 60 °C for 12 hours. The mould was removed and the protruding wires at the front were cut at the level of the acrylic wire guide. The cut surface was polished flat using an optical fibre polishing machine (MDC 12-GOD, Nanometer Technologies, CA, USA). The inset panel in Fig. 2 shows the arrangement of electrodes on the array recording surface.

C. Recording atrial electrograms during autonomic stimulation

The baroreflex was activated by pressure challenges created by driving the perfusion pump at maximum speed (220 rpm) for periods of between 1 and 5 s. Simultaneous recordings of atrial activation were made using the electrode array. The array was pressed against a region spanning the posterior right atrium and right atrial appendage. Unipolar extracellular electrograms were acquired (with respect to a remote reference) at a sampling frequency of 3 kHz (12-bit resolution) using a purpose-built mapping system (UnEmap, Auckland Uniservices Ltd., NZ). Electrograms were adjusted off-line to remove baseline drift as previously described [10] and filtered to suppress noise by using a Sovitzky-Golay filter (order 3, window size 5) implemented in Matlab (Mathworks, MA, USA).

D. Mapping activation times

The aggregate behaviour of all electrodes in the array was used as the basis for automatically detecting atrial beats. The root mean square (V_{RMS}) voltage of all electrograms for a given recording was calculated using the relationship:

$$V_{RMS}(t) = \sqrt{\frac{\sum_{i=1}^{n} v_i{}^2(t)}{n}}, \qquad (1)$$

where $v_i(t)$ is the potential of the electrogram i at time t and n is the total number of electrograms. A moving average over a 5 point window was applied to suppress noise and produce a smoothed RMS voltage ($\hat{V}_{RMS}$). Curvature of the

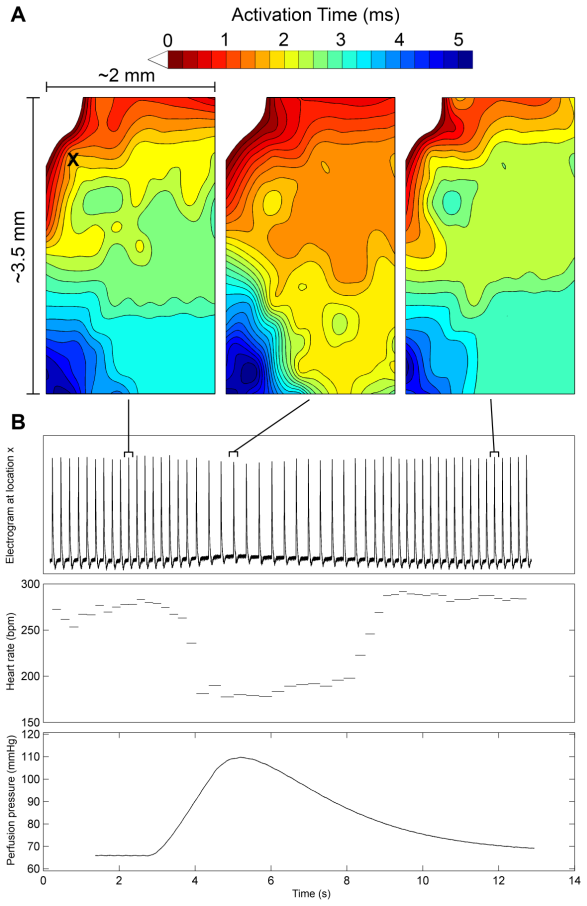

Fig. 3. **Baroreflex induced changes in heart rate and activation sequence.** Panel A contains activation time maps produced from beats prior to, during and following a transient increase in perfusion pressure. Panel B contains an electrogram trace from a representative electrode (at location marked X in Panel A), instantaneous heart rate and mean perfusion pressure.

smoothed waveform (*Curvature*) was calculated using the equation [11]:

$$Curvature(t) = \frac{|\frac{d^2\hat{V}_{RMS}}{dt^2}|}{\left(1+\left(\frac{d\hat{V}_{RMS}}{dt}\right)^2\right)^{\frac{3}{2}}}, \qquad (2)$$

Peaks in the dimensionless curvature waveform delineate significant deviations of the $\hat{V}_{RMS}$ from baseline. A window bounded by the first and last major curvature peaks was defined for each beat. Curvature peaks were detected using a threshold set to the mean curvature plus 3 standard deviations of the curvature during electrical quiescence. The time derivative ("slope") during each beat window was calculated using a least-square, cubic polynomial fit of a 5 point window centered about the time of interest. The time of maximum positive slope during a given beat window was defined as the activation time (AT) for each electrode. ATs were normalised to the earliest activation for a given beat. Maps were produced by fitting a surface to the ATs using linear interpolation on a triangular mesh [12].

III. Results and Discussion

Stimulation of the arterial barorecepters by transiently increasing PP caused a reflex reduction in heart rate and induced changes in atrial activation times that were detectable using the electrode array. Fig. 3 exhibits representative atrial activation maps produced from beats before, during and after baroreflex activation. Activation spread faster across the majority of the recording area during the baroreflex response in this experiment as evidenced by reduced activation times for all but the electrodes at the lower left. The electrodes on the lower left were slower to activate during the baroreflex response. The effects of baroreflex activation on atrial activation times were reversed once PP returned to baseline. As baroreflex activation results in an increase in vagal activity, the decrease in activation times we have observed are consistent with increases in atrial conduction velocity observed by others during direct vagal stimulation [3]. However, comparing individual beats may accentuate differences in activation times under different levels of autonomic activity. In addition, our initial data indicates there is some degree of uncertainty associated with the determination of activation times due to the presence of significant fractionation.

Achieving and maintaining adequate perfusion of the brainstem throughout the experiment is crucial for continuous viability of the preparation. This is done by increasing vascular resistance pharmacologically using the vasoconstrictor vasopressin and adjusting the perfusion pump flow rate to optimise the phrenic nerve burst duration and frequency. There is an opportunity to partially automate this process by using a machine learning approach which may significantly improve the duration of viability of preparations.

We have described an experimental set-up that enables the recording of atrial electrograms during endogenous baroreflex activation. This is a crucial step towards investigating the influence of baroreflex activation on the formation of atrial arrhythmias. Other preparations used to investigate autonomic mediated arrhythmias such as Langendorff perfused whole innervated hearts [13] or isolated superfused atrial tissue [14] are limited to pharmacological or direct nerve stimulation to modulate autonomic activity. Utilisation of the WHBP enables inherently more physiological autonomic stimulation regimes. Often studies *in vivo* induce baroreflex activation through the infusion of intraveneous phenylephrine. Phenylephrine has recently been shown to cause direct adrenergic effects on atrial electrophysiology that confound its baroreflex mediated effects [15]. We avoid this entirely by activating the baroreflex directly using pressure challenges. Furthermore, our set-up affords more complete characterization of the baroreflex response through control of baseline PP, and the maximum magnitude and rate of rise during pressure challenges. We intend to also compare the effects of baroreflex activation and direct electrical stimulation of the vagus nerves. Not limited to the baroreflex, this experimental set-up can be used to investigate atrial arrhythmia development under other autonomic reflexes, such

as via peripheral chemoreceptors and somatic nociceptors [16]. While this preparation provides a powerful test-bed it is limited to the study of animals up to 110 g in weight. More parallel pathways within the vascular network of preparations derived from larger animals make it very difficult to maintain adequate PP at reasonable flow rates [17].

This work will be extended to characterize the effects of baroreflex mediated nerve activity on the heterogeneity of atrial activation, repolarisation and regional effective refractory periods in a representative group of normal animals. Burst pacing could be used to induce AF to determine the influence of baroreflex activation on AF duration and dominant frequency [18]. In practice however, it is difficult to induce AF of significant duration in normal rats owing to the limitations imposed on potential re-entrant circuits by the small size of rat atria. We are also seeking to characterize any regional variation in the density of cholinergic and adrenergic nerve fibres within tissue from which atrial electrograms have been recorded. This is being done through extended volume confocal imaging [19] of whole atrial segments labeled with nerve specific antibodies. There are studies that indicate spatial heterogeneity of cholinergic nerves across the atria may cause the variations in refractoriness observed under vagal stimulation [3], [20]. However, more detailed experiments are required to elucidate the contribution of nerve structure relative to other factors that may play a part such as variations in the density of muscarinic receptors or acetylcholinesterase. It is clear the pulmonary veins (PVs) play a significant role in triggering paroxysmal AF [5]. Furthermore, prolongation of repolarisation in the PVs and posterior region of the left atrium in response to vagal stimulation could provide a substrate for AF [21]. However, permanent AF involves a wider range of substrates and triggers that are thought to be influenced by autonomic inputs to regions of the right atrium as well [5]. The longer term objectives of this work are to extend the image based analysis of nerve distribution to atrial tissue from structurally diseased hearts prone to permanent AF. The experimental set-up described will provide an important tool for assessing the functional implications of nerve structural remodeling.

IV. Acknowledgements

This work was funded by the Health Research Council of New Zealand. J. L. Ashton was supported by funding from the Freemasons Charity, the Todd Foundation and Heart Foundation of New Zealand.

References

[1] P. Coumel, "Paroxysmal Atrial Fibrillation: A Disorder of Autonomic Tone?" *European Heart Journal*, vol. 15, no. suppl A, pp. 9–16, Apr. 1994.

[2] A. Y. Tan, S. Zhou, M. Ogawa, J. Song, M. Chu, H. Li, M. C. Fishbein, S.-F. Lin, L. S. Chen, and P.-S. Chen, "Neural Mechanisms of Paroxysmal Atrial Fibrillation and Paroxysmal Atrial Tachycardia in Ambulatory Canines," *Circulation*, vol. 118, no. 9, pp. 916–925, 2008.

[3] L. Liu and S. Nattel, "Differing sympathetic and vagal effects on atrial fibrillation in dogs: role of refractoriness heterogeneity," *American Journal of Physiology-Heart and Circulatory Physiology*, vol. 273, no. 2, pp. H805–816, 1997.

[4] J. Ng, R. Villuendas, I. Cokic, J. E. Schliamser, D. Gordon, H. Koduri, B. Benefield, J. Simon, S. N. P. Murthy, J. W. Lomasney, J. A. Wasserstrom, J. J. Goldberger, G. L. Aistrup, and R. Arora, "Autonomic Remodeling in the Left Atrium and Pulmonary Veins in Heart Failure: Creation of a Dynamic Substrate for Atrial Fibrillation," *Circulation: Arrhythmia and Electrophysiology*, vol. 4, no. 3, pp. 388–U209, 2011.

[5] U. Schotten, S. Verheule, P. Kirchhof, and A. Goette, "Pathophysiological Mechanisms of Atrial Fibrillation : A Translational Appraisal," *Physiological Reviews*, vol. 91, no. 1, pp. 265–325, 2011.

[6] S. Oh, Y. H. Zhang, S. Bibevski, N. F. Marrouche, A. Natale, and T. N. Mazgalev, "Vagal denervation and atrial fibrillation inducibility: Epicardial fat pad ablation does not have long-term effects," *Heart Rhythm*, vol. 3, no. 6, pp. 701–708, 2006.

[7] L. Calò, M. Rebecchi, L. Sciarra, L. De Luca, A. Fagagnini, L. M. Zuccaro, P. Pitrone, S. Dottori, M. Porfirio, E. de Ruvo, and E. Lioy, "Catheter ablation of right atrial ganglionated plexi in patients with vagal paroxysmal atrial fibrillation." *Circulation: Arrhythmia and Electrophysiology*, vol. 5, no. 1, pp. 22–31, Feb. 2012.

[8] Y. J. Chen, C. T. Tai, C. W. Chiou, Z. C. Wen, P. Chan, S. H. Lee, and S. A. Chen, "Inducibility of atrial fibrillation during atrioventricular pacing with varying intervals: role of atrial electrophysiology and the autonomic nervous system." *Journal of Cardiovascular Electrophysiology*, vol. 10, no. 12, pp. 1578–85, Dec. 1999.

[9] J. F. R. Paton, "A working heart-brainstem preparation of the mouse," *Journal of Neuroscience Methods*, vol. 65, no. 1, pp. 63–68, 1996.

[10] V. S. Chouhan and S. S. Mehta, "Total removal of baseline drift from ECG signal," *Proceedings of the International Conference on Computing: Theory and Applications, ICCTA.*, pp. 512–515, 2007.

[11] M. S. Fuller, G. Sandor, B. Punske, B. Taccardi, R. S. MacLeod, P. R. Ershler, L. S. Green, and R. L. Lux, "Estimates of repolarization dispersion from electrocardiographic measurements," *Circulation*, vol. 102, no. 6, pp. 685–691, 2000.

[12] J. D'Errico, "Surface fitting using gridfit," 2005. [Online]. Available: http://www.mathworks.com/matlabcentral/fileexchange/8998-surface-fitting-using-gridfit

[13] G. A. Ng, R. Mantravadi, W. H. Walker, W. G. Ortin, B. R. Choi, W. de Groat, and G. Salama, "Sympathetic nerve stimulation produces spatial heterogeneities of action potential restitution," *Heart Rhythm*, vol. 6, no. 5, pp. 696–706, 2009.

[14] J. K. Choate and R. Feldman, "Neuronal control of heart rate in isolated mouse atria." *American journal of physiology. Heart and circulatory physiology*, vol. 285, no. 3, pp. H1340–6, Sept. 2003. [Online]. Available: http://www.ncbi.nlm.nih.gov/pubmed/12738615

[15] J. Ng, R. S. Passman, R. Arora, A. H. Kadish, and J. J. Goldberger, "Paradoxical change in atrial fibrillation dominant frequencies with baroreflex-mediated parasympathetic stimulation with phenylephrine infusion." *Journal of Cardiovascular Electrophysiology*, vol. 23, no. 10, pp. 1045–50, Oct. 2012.

[16] J. F. R. Paton, P. Boscan, A. E. Pickering, and E. Nalivaiko, "The yin and yang of cardiac autonomic control: Vago-sympathetic interactions revisited," *Brain Research Reviews*, vol. 49, no. 3, pp. 555–565, 2005.

[17] A. E. Pickering and J. F. R. Paton, "A decerebrate, artificially-perfused in situ preparation of rat: Utility for the study of autonomic and nociceptive processing," *Journal of Neuroscience Methods*, vol. 155, no. 2, pp. 260–271, 2006.

[18] S.-J. Kim, S. C. M. Choisy, P. Barman, H. Zhang, J. C. Hancox, S. A. Jones, and A. F. James, "Atrial remodeling and the substrate for atrial fibrillation in rat hearts with elevated afterload." *Circulation. Arrhythmia and Electrophysiology*, vol. 4, no. 5, pp. 761–9, Oct. 2011.

[19] G. B. Sands, D. A. Gerneke, D. A. Hooks, C. R. Green, B. H. Smaill, and I. J. Legrice, "Automated imaging of extended tissue volumes using confocal microscopy." *Microscopy Research and Technique*, vol. 67, no. 5, pp. 227–39, Aug. 2005.

[20] R. Arora, J. S. Ulphani, R. Villuendas, J. Ng, L. Harvey, S. Thordson, F. Inderyas, Y. Lu, D. Gordon, P. Denes, R. Greene, S. Crawford, R. Decker, A. Morris, J. Goldberger, and A. H. Kadish, "Neural substrate for atrial fibrillation: implications for targeted parasympathetic blockade in the posterior left atrium," *American Journal of Physiology-Heart and Circulatory Physiology*, vol. 294, no. 1, pp. H134–144, 2008.

[21] R. Arora, J. Ng, J. Ulphani, I. Mylonas, H. Subacius, G. Shade, D. Gordon, A. Morris, X. He, Y. Lu, R. Belin, J. J. Goldberger, and A. H. Kadish, "Unique autonomic profile of the pulmonary veins and posterior left atrium," *Journal of the American College of Cardiology*, vol. 49, no. 12, pp. 1340–1348, 2007.